Control of Thymic T Cell Maturation, Deletion and Egress by the RNA-Binding Protein HuR[1]

Olympia Papadaki,* Stavros Milatos,* Sofia Grammenoudi,* Neelanjan Mukherjee,† Jack D. Keene,† and Dimitris L. Kontoyiannis[2]*

HuR emerged as a posttranscriptional regulator of mRNAs involved in cellular control, stress, and immunity but its role in governing such responses remains elusive. In this study, we assessed HuR's role in the staged progression of thymic T cell differentiation by means of its genetic ablation. Mice with an early deletion of HuR in thymocytes possess enlarged thymi but display a substantial loss of peripheral T cells. We show that this discordant phenotype related to specific defects in thymic cellular processes, which demonstrated HuR's involvement in: 1) intrinsic checkpoint signals suppressing the cell cycle of immature thymocyte progenitors, 2) TCR and antigenic signals promoting the activation and positive selection of mature thymocytes, 3) antigenic and death-receptor signals promoting thymocyte deletion, and 4) chemokine signals driving the egress of postselection thymocytes to the periphery. The cellular consequences of HuR's dysfunction were underlined by the aberrant expression of selective cell cycle regulators, TCR, and death-receptor signaling components. Our studies reveal the signal-dependent context of HuR's cellular activities in thymocytes and its importance in the generation of a physiological T cell pool. ***The Journal of Immunology,*** **2009, 182: 6779–6788.**

Thymic T cell development involves discrete stages of differentiation, activation, death, and migration aiming to provide a T cell repertoire against invasion while maintaining tolerance to self. Double-negative (DN)[3] progenitors ($CD4^-CD8^-$) entering the thymic cortex from the bone marrow proceed through four differentiation stages to yield cells competent for antigenic stimulation. In the case of conventional T cells, this is achieved by the somatic recombination of TCRβ genes, the elimination of aberrant rearrangements, and the association of the TCRβ-chains with the invariant TCRα-chain. This pre-TCR complex signals DN cells to expand and become $CD4^+CD8^+$ double-positive (DP) cells (1). DP cells rearrange their TCRα locus and progressively express surface TCRα/β for interaction with MHC-presented Ags on the thymic epithelium. The qualitative and quantitative features of these interactions guide the selection of nonself reacting $CD4^+$ or $CD8^+$ single-positive (SP) thymocytes (2). Nominal or strong autoreactive interactions cause elimination by neglect or negative selection, respectively; moderate interactions lead to positive selection. In parallel, an array of cytokine/chemokine signals define the thresholds of these interactions and facilitate thymocyte movements from the cortex to the medulla and peripheral blood (3, 4). These staged events require the precise orchestration of gene expression programs governed by genetic, epigenetic, and transcriptional mechanisms.

Posttranscriptional mechanisms of mRNA use may also affect thymocyte development because they contribute to as much as 50% of T cell-specific gene expression changes during activation (5). However, the *trans*-acting factors regulating these changes have not been well studied. Such factors include the RNA-binding proteins (RBPs) that determine mRNA maturation, localization, stability, and translation (6). This type of control is particularly stringent in mRNAs that possess adenylate and/or uridylate-rich elements and frequently encode cytokines, signaling molecules, and oncoproteins (7). Within the selective set of RBPs recognizing adenylate and/or uridylate-rich elements, HuR (or HuA) emerged as a pleiotropic modulator of mRNA use. HuR contains RNA recognition motifs with an affinity for a U-rich motif and it is the only ubiquitous member of the otherwise neuronal Elavl/Hu family (8). HuR shuttles between the nucleus and the cytoplasm via interactions with nuclear export/import adaptor proteins (9). In the cytoplasm, HuR can affect mRNA stability and/or translation (8, 10–12) via complex interplays with other RBPs, such as hnRNPD/AUF1, TTP, BRF1 and KSRP, as well as microRNAs (13, 14). Recent data suggest that HuR's functions can be controlled by posttranslational modifications like phosphorylation, methylation, and cleavage (15–18). Furthermore, HuR:RNA immunoprecipitations demonstrated that, in vivo, HuR associates with mRNAs that are relevant to a certain cellular response (6, 14), suggesting that its functions may vary in a tissue and signal-specific manner. Such an example has been provided for macrophages where HuR's overexpression suppressed the translation of specific inflammatory mRNAs and attenuated acute inflammatory reactions (10). HuR's involvement in adaptive immunity has been inferred by its interactions with mRNAs encoding CD3ζ, TNF, CD95/Fas, APRIL, CD40L, GM-CSF, IL-3, IL-4, and IL-13 (19–25), but these interactions were not informative on HuR's control over multiparametric immune responses. The obligatory deletion of HuR in the

*Institute of Immunology, Biomedical Sciences Research Centre "Alexander Fleming", Vari, Greece; and †Department of Molecular Genetics & Microbiology, Duke University Medical Center, Durham, NC 27710

Received for publication February 3, 2009. Accepted for publication March 31, 2009.

The costs of publication of this article were defrayed in part by the payment of page charges. This article must therefore be hereby marked *advertisement* in accordance with 18 U.S.C. Section 1734 solely to indicate this fact.

[1] This work was supported by funding under the Sixth Research Framework Programme of the European Union, Project MUGEN NoE LSHG-CT-2005-005203 (www.mugen-noe.org) and the Hellenic Secretariat for Research and Technology Grants GSRT-PENED2003-394 and GSRT-PENED2003-264.

[2] Address correspondence and reprint requests to Dr. Dimitris L. Kontoyiannis, Institute of Immunology, Biomedical Sciences Research Centre "Alexander Fleming", 34 Al. Fleming Street, 166 72 Vari, Greece. E-mail address: kontoyiannis@fleming.gr

[3] Abbreviations used in this paper: DN, double negative; Cdk, cyclin-dependent kinase; DP, double positive; RBP, RNA-binding protein; R-IP, RNA-immunoprecipitation; RTE, recent thymic emigrant; SP, single positive.

www.jimmunol.org/cgi/doi/10.4049/jimmunol.0900377

mouse blocked embryonic development, thus prohibiting the assessment of its involvement in immune processes (26). The analysis of these embryos highlighted HuR's control over developmental morphogenesis, but it could not reveal its effect on fundamental cellular responses. The staged progression of thymocyte development is an ideal process for assessing both HuR's cellular functions and its role in adaptive immunity. In this study, we restricted HuR's deletion in mouse thymocytes and revealed its control over distinct signal-dependant cellular responses.

Materials and Methods

Mice

The generation of the floxed *Elavl1* allele (*Elavl1^{fl}*) was described in (26). *Elavl1$^{fl/fl}$* mice were backcrossed to C57BL/6J background for at least five generations. Additional transgenic mice were provided by J. D. Marth (*LckCre*; University of California, San Diego, CA) (27), D. Kioussis (*F5-TCR*; National Institute for Medical Research, London, United Kingdom) (28, 29), B. Malissen (*TgHYTCR*; Centre d'Immunologie de Marseille-Luminy, Université de la Méditerrannée, Marseille, France) (30), and G. Kollias (*RAG1$^{-/-}$* Biomedical Sciences Research Centre (BSRC) "Alexander Fleming", Vari, Greece). All transgenic mice were crossed to C57BL/6 for more than nine generations. Congenic C57BL/6–CD45.1 mice were provided by A. Potocnik (National Institute for Medical Research, London, United Kingdom). All mice were bred and maintained in the animal facilities of the BSRC "Alexander Fleming" under specific pathogen-free conditions. Experiments on live animals were approved by the Hellenic Ministry of Rural Development (Directorate of Veterinary Services) and by BSRC Alexander Fleming's Animal Research and Ethics Committee for compliance to Federation of European Laboratory Animal Science Associations' regulations.

Cell isolation and stimulation

Cells from thymus, peripheral blood, spleen, and mesenteric lymph nodes were isolated using standard procedures. For stimulation, cells were cultured in complete RPMI 1640 with 2.5% FBS. For TCR-induced activation of kinases, thymocytes were first incubated on ice with anti-CD3 or anti-CD3/CD28 (0.5 μg/ml each) and then were cross-linked with goat anti-hamster IgG (40 μg/ml) at 37°C for 5 min. For HuR detection during apoptosis, thymocytes were stimulated with anti-Fas (100 ng/ml) in the presence of Cycloheximide (0.1 μM; Sigma-Aldrich) or Dexamethasone (100 nM; Sigma-Aldrich). For the chemokine-induced translocation of HuR, thymocytes were stimulated with CCL21 or SDF-1 (10 ng/ml; PeproTech) for 3 h.

Flow cytometry and sorting

For surface Ags, staining was performed via standard procedures. For intracellular Ags, cells were processed with Cytofix and Cytoperm (BD Biosciences) according to the manufacturer's protocol. The flow cytometric detection of HuR was achieved by a biotin-conjugated anti-HuR Ab (3A2; sc5261) generated by Santa Cruz Biotechnology upon request, whereas the mIgG1 isotype control (IC002B) was purchased from R&D Systems. The remaining Abs for flow cytometry were purchased from BD Biosciences, with the exception of EDG-1 (Santa Cruz Biotechnology); CD4, T3.70 (HY-TCR), and CXCR4 (eBioscience); CCR7, CD45.1, and CD45.2 (BioLegend); Kruppel-like transcription factor 2 (Chemicon International); and biotinylated DR3 (R&D Systems). Stained cells were analyzed with FACS Canto II or sorted with using FACSVantage SE flow cytometer (BD Biosciences). Data were acquired with CellQuest or FACSDiva software (BD Biosciences) and analyzed using FlowJo (Tree Star). DN thymocytes were sorted as CD4$^-$CD8$^-$CD11b$^-$CD45R/B220$^-$CD49β^-TER119$^-$ after enrichment by negative selection using the IMag mouse CD4 lymphocyte enrichment set (BD Biosciences) followed by FACS sorting.

Cell cycle and proliferation assays

For in vivo cell cycle analysis, 8–10-wk-old mice were injected i.p. with 100 μl of 10 mg/ml BrdU (Sigma-Aldrich) and killed after 60 min. For BrdU staining, 5–10 $\times$ 10^6 thymocytes were first stained for surface markers, then treated with Cytofix (BD Biosciences) for 1 h on ice and finally incubated with FastImmune anti-BrdU with DNase (BD Biosciences) for 1 h at room temperature. After DNA staining with 7-amino-actinomycin (5 μg/ml; Sigma-Aldrich), cells were analyzed by flow cytometry. For ex vivo proliferation assays, thymocytes were cultured in triplicates in microtiter plates (3 $\times$ 10^4/well) and stimulated with plate-bound anti-CD3 (10 μg/ml), anti-CD3 plus anti-CD28 (10 μg/ml; BioLegend), or soluble PMA (10 ng/ml; Sigma-Aldrich) and ionomycin (500 ng/ml; Calbiochem). At 72 h, wells were pulsed with 1μCi [^{3}H]thymidine and 6 h later they were harvested onto glass membranes for scintillation counting.

Competitive repopulation assay

Bone marrow cells were isolated from femurs/tibia of 6–8-wk-old male CD45.1 (competitor), CD45.2 *LckCre$^+$ Elavl1$^{fl/+}$* (control), and CD45.2 *LckCre$^+$ Elavl1$^{fl/fl}$* (test) mice. The representation of bone marrow progenitors was similar among genotypes as assessed by flow cytometry. Following purification, 4 $\times$ 10^5 cells containing a 1/1 mixture from each genotype were injected into the tail-vain of irradiated (800 Gy), age-matched male CD45.2 RAG1-deficient mice. Reconstitution was monitored by flow cytometric analysis of peripheral blood. Mice were killed past the age of 8 wk for the estimation of the CD45.1/CD45.2 percentages in the thymus and peripheral lymphoid organs via flow cytometry. The corresponding CD45.2 percentages were normalized to CD45.1 and expressed as ratios of CD45.2 test:CD45.2 control.

Migration and chemotaxis assays

Intrathymic FITC (10 μg/thymic lobe; Sigma-Aldrich) injections were performed as described (31). Chemotactic assays were performed in 5 μm Transwell filters (Corning), for 3 h to S1P (Avanti Polar Lipids), CCL21, CXCL12/SDF-1 (PeproTech), or medium in the bottom chamber and enumerated by flow cytometry, as described (32). Assays were performed in duplicate for each concentration, and were repeated using cells from a minimum of two different animals per genotype. Values were normalized to passively migrating DP cells.

Assays for T cell apoptosis

For TCR-induced thymocyte apoptosis, 6–7 wk-old mice were injected i.p with either 25 μg anti-CD3 (145 2C11) or saline at 0 and 24 h. Twenty-four hours after the last injection, thymocytes were enumerated by flow cytometry. For the apoptotic response of F5 TCR-transgenic thymocytes, 6-wk-old mice were injected i.p. daily for 4 days with either saline or 20–50 nM NP68 peptide in saline. The NP68 peptide was the 9-mer Ala-Ser-Asn-Glu-Asn-Met-Asp-Ala-Met (366–374) from the nucleoprotein of influenza virus A/NT/60/68. On day 4, thymi, spleens, and mesenteric lymph nodes were removed for flow cytometry. For ex vivo apoptotic assays, 5 $\times$ 10^6/ml thymocytes from 6–7-wk-old mice were cultured in plates coated with 1 μg/ml CD3 mAb and either 2 or 20 μg/ml CD28 mAb. Cells were harvested 24 h later and stained with anti-CD4, anti-CD8, and Annexin V for flow cytometry. For Fas-induced apoptosis, thymocytes were stimulated with various doses of anti-Fas Ab (Jo-2, 0–1000 ng/ml) plus 0.1 μM cycloheximide in RPMI 1640. Apoptosis in DP thymocytes was assessed 18 h later by Annexin V staining and flow cytometry.

Protein analysis via immunoblots

Whole-cell lysates were prepared in RIPA buffer, whereas nuclear and cytoplasmic extracts were prepared with the NE-PER reagent (Pierce). Equimolar amounts of protein were analyzed on SDS-containing polyacrylamide gels and blotted onto nitrocellulose membranes (Schleicher & Schuell Microscience). Probing Abs included: HuR (3A2), procaspase-3 (L-18), actin (C-11), p27 (F-8), p21 (F-5), U1snRNP (C-18), Lck (3A5), ZAP70 (1E7.2), and PKCθ (C18) (all obtained from Santa Cruz Biotechnology); cleaved caspase-3 (Asp175), caspase-8, p-Src (Tyr 416, recognizing Lck phosphorylated at Tyr 394), pZAP70 (Tyr 319), pPKCθ (Thr538) and p53 (1C12) (all obtained from Cell Signaling Technology). Primary Abs were detected with HRP-conjugated secondary Abs (Southern Biotechnologies) and the ECL+ substrate (Amersham).

RNA analysis and immunoprecipitation

Total RNA was extracted from thymocytes using the RiboPure Kit (Ambion) according to the manufacturer's instructions. RNA-immunoprecipitation (R-IP) assays were performed as previously described (10) using agarose conjugated anti-HuR (3A2; sc5261) or control IgG (sc2343) Abs generated by Santa Cruz Biotechnologies upon request. For RT-PCR analyses, 5–10 μg of cellular RNA were used for cDNA synthesis with Moloney murine leukemia virus reverse transcriptase (Promega). cDNAs were used for quantitative RT-PCR performed using Platinum SYBR Green qPCR SuperMix UDG (Invitrogen) on RotorGene 6000 machine (Corbett Research). Expression was normalized to B2 microglobulin and L32 mRNAs. Relative expression was calculated as the fold difference to control values that were assigned an arbitrary expression value of 1, using BioRad RelQuant or REST 2005 (Corbett Research). Control values were assigned an arbitrary expression value of 1. In all cases data were derived from three mice, groups, or genotypes analyzed in triplicate and summing up to nine

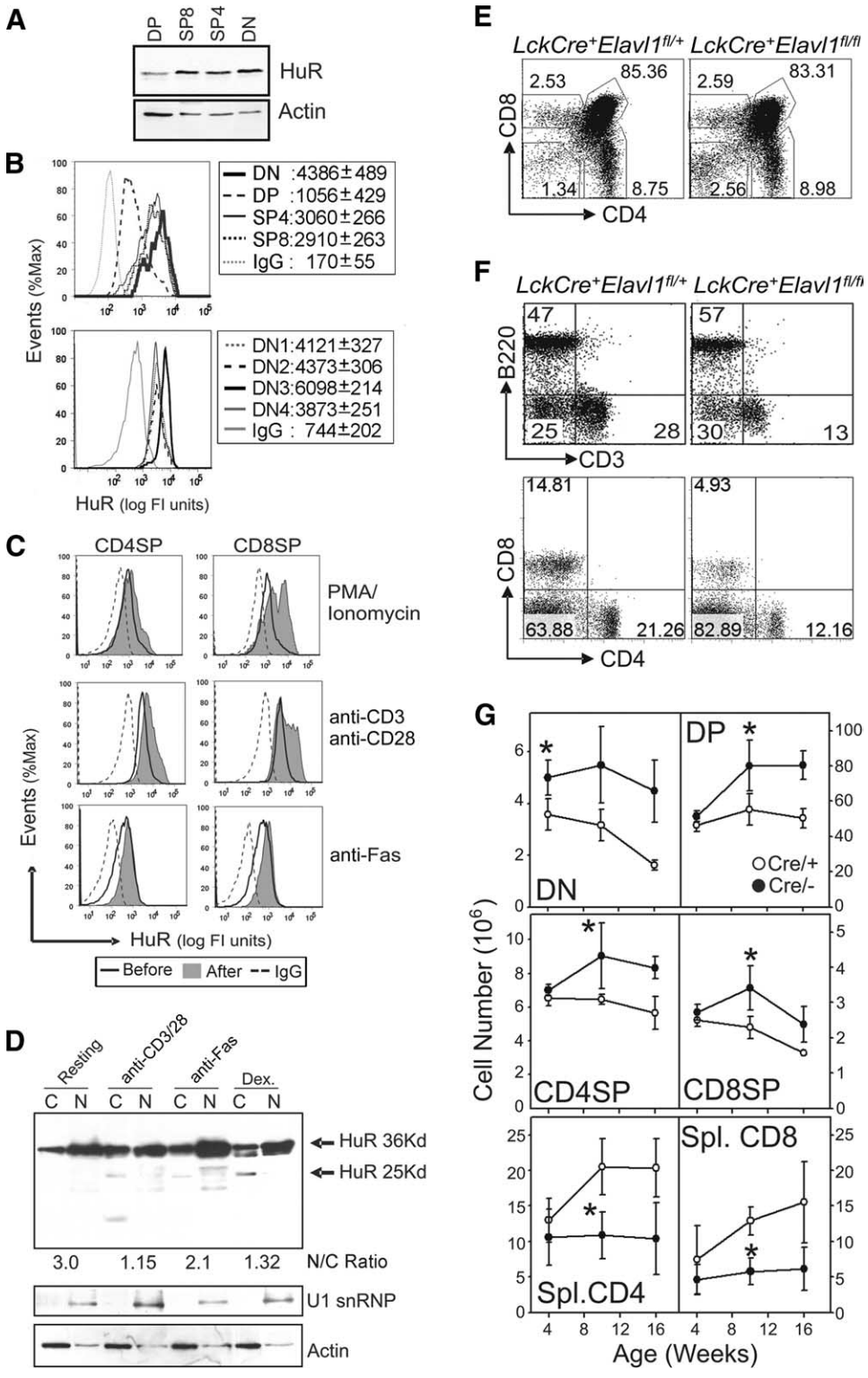

FIGURE 1. Responses of murine thymocyte HuR and effects of its ablation in T cell composition. *A*, Detection of HuR protein in sorted mouse thymocyte subsets via immunoblots with actin as a loading control. *B*, Flow cytometric detection of HuR in total mouse thymocyte subsets or in DN subsets. Values (±SD) are mean fluorescence intensity values from three experiments. *C*, Flow cytometric detection of HuR in thymocytes responding to mitogens and anti-CD3/anti-CD28 for 5 h or anti-Fas for 18 h. *D*, Detection of full-length (36Kd) and cleaved (25Kd) HuR in nuclear (N) or cytoplasmic (C) extracts from thymocytes stimulated with TCR agonists, anti-Fas, or Dexamethasone. Ratios denote representative changes in nuclear vs cytoplasmic HuR. U1snRNP marks nuclear extracts and Actin is the loading control. Flow cytometry of *LckCre*$^+$ *Elavl1*$^{fl/+}$ and *LckCre*$^+$ *Elavl1*$^{fl/fl}$ thymocyte subsets assessed by CD4/CD8 staining at 6 wk of age (*E*) or splenocyte subsets assessed by B220 (B cells), CD3 (total T cells), or CD4/CD8 staining at 12 wk of age (*F*). *G*, Age-dependant changes in *LckCre*$^+$ *Elavl1*$^{fl/+}$ and *LckCre*$^+$ *Elavl1*$^{fl/fl}$ thymocytes and splenic T cells by means of their CD4/CD8 expression. Data (±SD) derived from $n = 6$–10 mice/group/time point. $*$, $p < 0.05$.

independent reactions for each measurement. Primer sequences, microarray analyses, and meta-analyses are described in *Extended Methods*.[4] The microarray data was submitted to the Gene Expression Omnibus (http://www.ncbi.nlm.nih.gov/geo) under the record number GSE9174.

Statistics

Unless otherwise indicated, Student's *t* test was used for statistical analysis. Results with a *p* value <0.05 were considered significant.

[4] The online version of this article contains supplemental material.

Results

Changes in thymocyte HuR during maturation and effects of its loss in T cell cellularity

To link HuR's functions to thymocyte responses, we first assessed its abundance in thymocyte subsets. The highest HuR content was detected in DN thymocytes, particularly in DN3 (CD25$^+$CD44$^-$) cells (Fig. 1, *A* and *B*), relating to TCRβ selection and pre-TCR signaling. HuR levels dropped in DP cells, but rose again in SP subsets, correlating to TCR signals driving thymocyte selection.

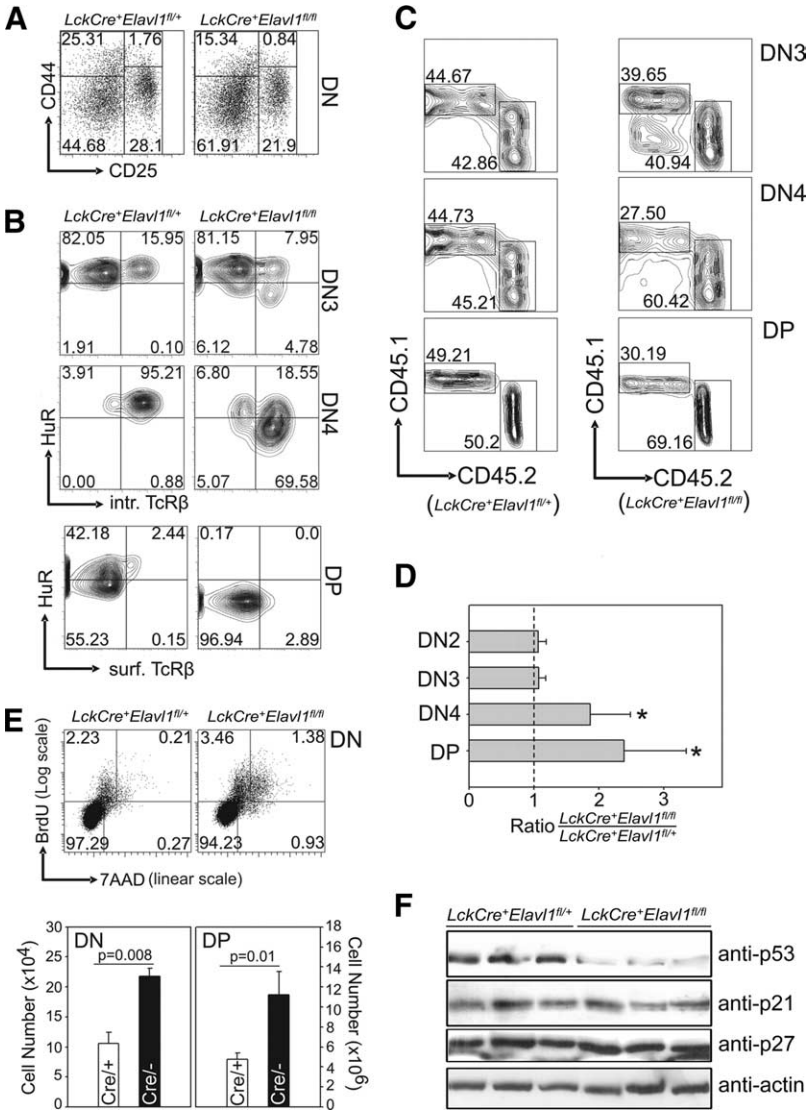

FIGURE 2. HuR$^-$ DN thymocytes show increased fitness due to accelerated cell cycle progression. *A*, Changes in *LckCre*$^+$ *Elavl1*$^{fl/+}$ and *LckCre*$^+$ *Elavl1*$^{fl/fl}$ DN thymocytes by means of their CD44/CD25 expression. *B*, Detection of HuR$^-$ cells in gated *LckCre*$^+$ *Elavl1*$^{fl/+}$ and *LckCre*$^+$ *Elavl1*$^{fl/fl}$ DN3, DN4, and DP thymocytes by means of their intracellular or surface TCRβ expression. Genotype composition of reconstituted thymi following competitive bone marrow transfers (*C*) and fitness of *LckCre*$^+$ *Elavl1*$^{fl/fl}$ DN and DP thymocytes in reconstituted thymi as ratios to *LckCre*$^+$ *Elavl1*$^{fl/+}$ cells normalized to competitor cells (*D*). Data ($\pm$SD) from $n = 5$–7 mice/group. $*$, $p < 0.05$. *E*, Cell cycle analysis of *LckCre*$^+$ *Elavl1*$^{fl/+}$ and *LckCre*$^+$ *Elavl1*$^{fl/fl}$ DN thymocytes at 1 h post-BrdU administration and detection of replicating cells (BrdU$^+$) relative to DNA content (7-amino-actinomycin; 7AAD). Percentage values for G0/G1 (2N DNA content), S (intermediate content), and G2/M (4N DNA content) cells are shown in the respective regions. The graph depicts the number of BrdU$^+$ cells in DN and DP subsets. Values ($\pm$SEM) and statistics derived from four mice/group. *F*, Immunoblots of p53, p21, and p27 proteins in extracts from sorted *LckCre*$^+$ *Elavl1*$^{fl/+}$ and *LckCre*$^+$ *Elavl1*$^{fl/fl}$ DN thymocytes. Shown are extracts from three independent isolates/genotype with actin as a quantifier.

(Fig. 1, *A* and *B*). TCR agonists (anti-CD3/CD28), mitogens (PMA/ionomycin), and apoptotic stimuli (anti-Fas) increased the levels of HuR in SP subsets, which contain high surface TCR (Fig. 1*C*). The same signals also elicited the strong cytoplasmic accumulation of thymocyte HuR (Fig. 1*D*), confirming observations on T cell lines (19). However, both TCR and apoptotic signals (CD95/Fas or corticosteroids) induced the cytoplasmic cleavage of HuR, which is known to induce apoptosome activation (Fig. 1*D*; Ref 18).

The differential response of HuR to thymocyte signals suggested that it may be involved in the cellular events driving thymocyte maturation. To reveal HuR's role in these events, we induced the Cre-mediated inactivation of its murine *Elavl1* locus in thymocytes by crossing *LckCre* transgenic mice to mice bearing an inactivatable, loxP-containing allele (*Elavl1*^{fl}; Supplemental Fig. 1) (26). Because monoallelic and compound heterozygote mutant thymocytes expressed comparable levels of HuR, we present *LckCre*$^+$ *Elavl1*$^{fl/+}$ as controls for *LckCre*$^+$ *Elavl1*$^{fl/fl}$. The recombination of the *Elav1l*^{fl} locus and the loss of HuR protein were consistent among different *LckCre*$^+$ *Elavl1*$^{fl/fl}$ thymi, whereas intracellular flow cytometry validated that >90% of *LckCre*$^+$ *Elavl1*$^{fl/fl}$ TCR$\alpha\beta^+$ thymocytes and peripheral T cells possessed a HuR-null (HuR$^-$) phenotype (Supplemental Fig. 1). At the age of 4 wk, mutant thymi contained a normal number of DP and SP thymocytes but increased numbers of DN cells (Fig. 1, *E* and *G*); however, at 10 wk, cellular increases extended to all thymocytes in *LckCre*$^+$ *Elavl1*$^{fl/fl}$ mice and persisted past this age, thus contributing to delays in thymic involution (Fig. 1*G* and not shown). In contrast, the peripheral T cell counts in these mice were progressively reduced to <50% of control values and were most prominently diminished in aged mice (Fig. 1, *F* and *G* and not shown). Thus, the loss of HuR in thymocytes disturbed the balanced representation of T cells in lymphoid organs, which could be due to aberrations in the staged progression of thymic T cell development.

HuR modulates the cell cycle of DN thymocytes

Hypercellular thymi may result from the defective control of DN cells, which provide the thymocyte pool for selection. In *LckCre*$^+$ *Elavl1*$^{fl/fl}$ thymi, HuR$^-$ cells were first detected between DN2 and DN3, coinciding to the emergence of intracellular TCRβ (Fig. 2*B*). The median ratio of HuR$^+$/HuR$^-$ cells at DN3 in mutant mice was 1.6:1.0 but changed dramatically in favor of HuR$^-$ cells at DN4 (1.0:4.0), accounting for increased DN4 counts and the predominance of HuR$^-$ cells in descendant immature SP, DP, and mature SP thymocytes as well as peripheral T cells (Fig. 2, *A* and *B* and supplemental Fig. 2). The progressive prevalence of HuR$^-$ T cells could be either due to the staged recombination of the *Elavl1* locus or to the increased fitness of HuR$^-$ cells. To determine which was

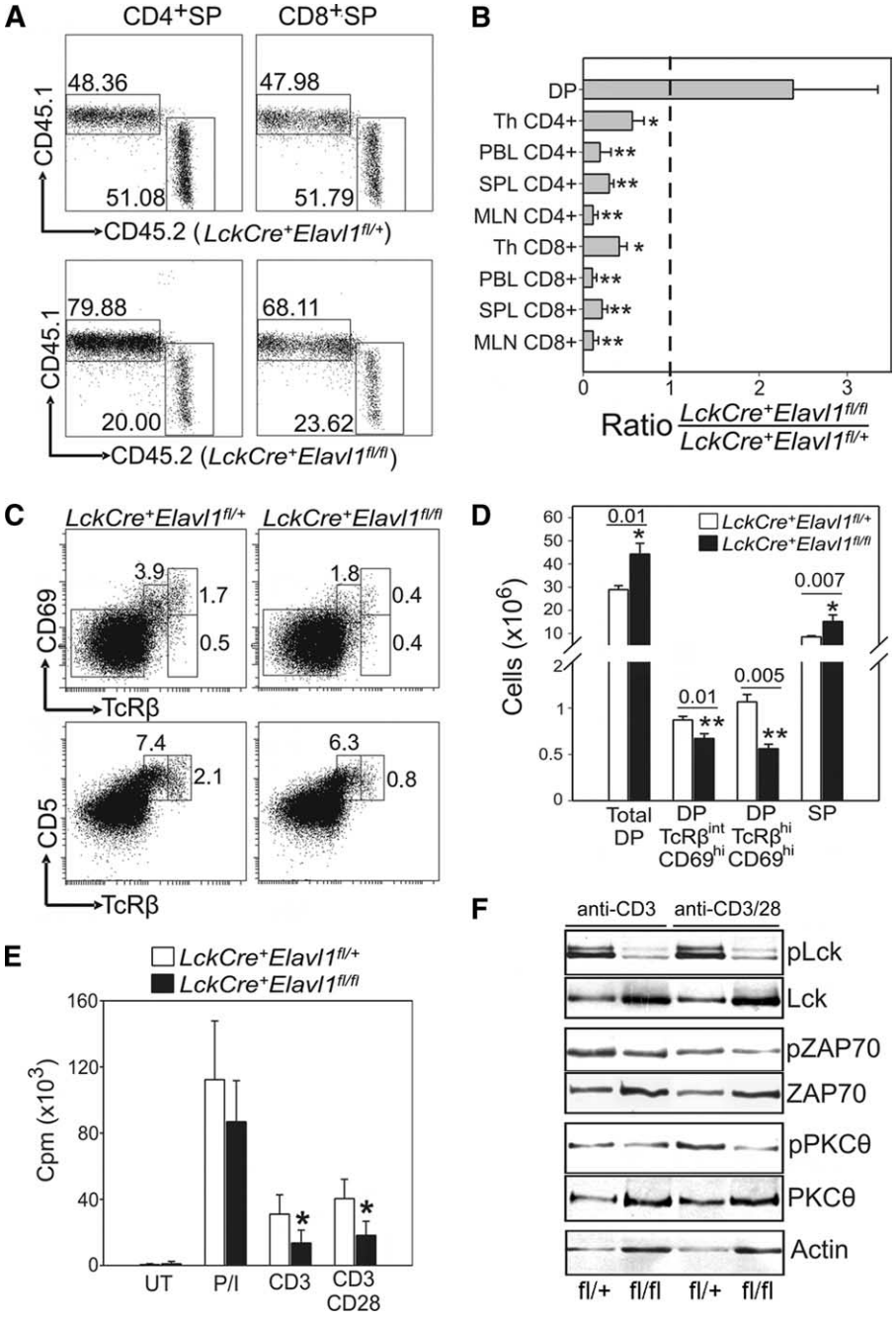

FIGURE 3. HuR$^-$ thymocytes show defects in positive selection and TCR signaling. Genotype composition of reconstituted SP thymocytes following competitive bone marrow transfers (*A*) and fitness of *LckCre*$^+$ *Elavl1*$^{fl/fl}$ DP/SP thymocytes (Th) and peripheral T cells from blood (PBL), spleen (SPL) and mesenteric lymph nodes (MLN) as a ratio to *LckCre*$^+$ *Elavl1*$^{fl/+}$ cells normalized to competitor cells (*B*). $*$ and $**$ denote significant differences from DP or SP thymocytes respectively ($p < 0.01$). *C* and *D*, Detection and enumeration of *LckCre*$^+$ *Elavl1*$^{fl/+}$ and *LckCre*$^+$ *Elavl1*$^{fl/fl}$ DP thymocytes initiating (TCRβ^{int}CD69^{high}) and undergoing (TCRβ^{high}CD69^{high}) positive selection relative to total DP and SP. Data ($\pm$SEM) from $n = 5$ mice/group. $*$, $p \leq 0.03$. *E*, Thymocyte proliferation assay in response to PMA/ionomycin, anti-CD3, and anti-CD3/CD28. Data (cpm $\pm$ SD) from [^{3}H]thymidine incorporation assays with $n = 4-6$ mice/group. $*$, $p < 0.01$. *F*, Detection of native and phosphorylated p56^{lck}, ZAP-70, and PKCθ in extracts from thymocytes pulsed with anti-CD3 and anti-CD3/CD28. Note the increased loading of *LckCre*$^+$ *Elavl1*$^{fl/fl}$ extracts (actin and native forms) that emphasizes the reduction in phosphorylated proteins.

the cause, we used competitive repopulation of the thymus in immunodeficient hosts to measure the fitness of mutant cells via their representation in each stage. CD45.1 bone marrow progenitors (competitor) were mixed either with CD45.2 *LckCre*$^+$ *Elavl1*$^{fl/+}$ (control) or CD45.2 *LckCre*$^+$ *Elavl1*$^{fl/fl}$ (test) progenitors and transplanted onto irradiated CD45.2 *RAG1*$^{-/-}$ mice. Injection of competitor with control progenitors resulted in the equal representation of descendant thymocyte subsets; in contrast, the mix of competitor with test progenitors was followed by the overrepresentation of *LckCre*$^+$ *Elavl1*$^{fl/fl}$ cells at DN4 and DP thymocytes (Fig. 2, *C* and *D*), suggesting that HuR controls the expansion of the pre-TCR-expressing immature thymocytes. To verify this, we assessed the proliferative competence of HuR$^-$ thymocytes by giving a pulse of BrdU in vivo, followed by cell cycle analysis. *LckCre*$^+$ *Elavl1*$^{fl/fl}$ thymi showed a clear increase in the number of BrdU$^+$ DN cells in the S or G2/M phases and their descendant DPs (Fig. 2*E*). The control of DN′s cell cycle is known to be achieved via a checkpoint that allows for DNA repair and elimination of aberrant TCRβ rearrangements and requires the activation of the p53 tumor suppressor and cyclin-dependent kinase (Cdk) inhibitors like p21 and p27. HuR is known to bind to p53, p21, and p27 mRNAs (11, 12, 33), but their steady state levels remained unaltered in sorted mutant DN cells (not shown). Similarly, the levels of p21 and p27 proteins were not grossly affected by HuR's loss; however, the p53 protein was reduced 3-fold in mutant DN cells (Fig. 2*F*). Thus, HuR controls the cell cycle progression of DN thymocytes during TCRβ selection relating to its effects on the expression of the p53 suppressor.

HuR regulates TCR signaling and positive selection

Our reconstitution experiments revealed additional defects that could not be observed in a noncompetitive environment. In contrast to HuR$^-$ DP thymocytes, their SP descendants were reduced

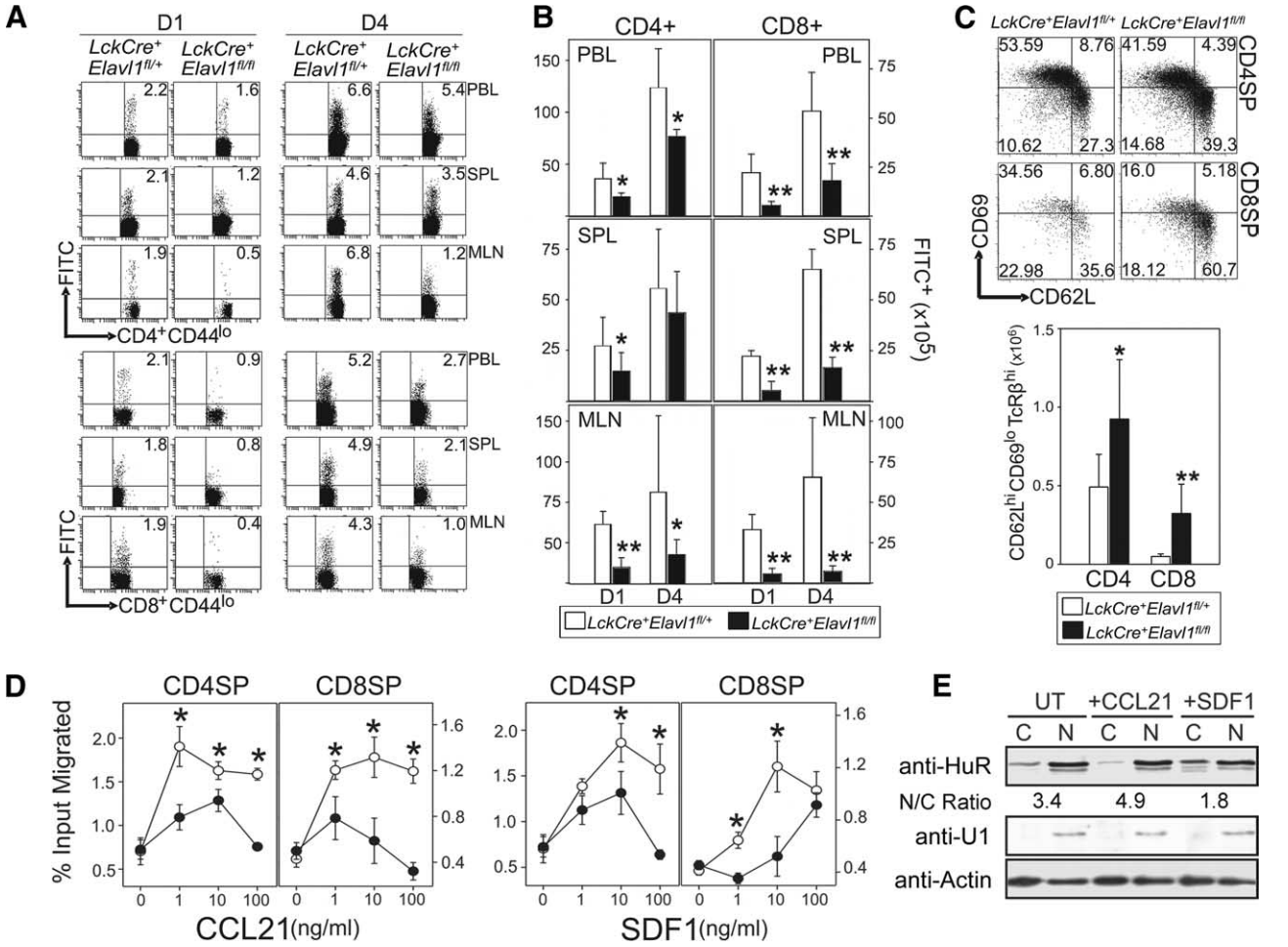

FIGURE 4. HuR$^-$ thymocytes show defects in thymocyte egress and chemotaxis. *A* and *B*, Detection and counting of FITC$^+$CD44^{low}, CD4$^+$, and CD8$^+$ RTEs in peripheral blood (PBL), spleen (SPL), and mesenteric lymph nodes (MLN) of 4-wk-old mice (n = 5–10/time point) at days 1 (D1) and 4 (D4) post-intrathymic FITC injection. *, $p < 0.05$ and **, $p < 0.001$. *C*, Detection and counting of migratory *LckCre$^+$ Elavl1$^{fl/+}$* and *LckCre$^+$ Elavl1$^{fl/fl}$*, TCRβ^{high} CD69^{low}CD62L^{high} SP thymocytes. Data (±SD) from n = 5 mice/group at 6–8 wk of age. *D*, Chemotactic response of SP thymocytes to CCL21 and SDF1 depicted as percentages of input SP cells that migrated to each chemokine normalized to the corresponding DP cells. Data from three independent experiments with n = 6 mice/genotype. *, $p < 0.01$. *E*, Nucleocytoplasmic distribution of HuR in proficient thymocytes stimulated with CCL21 or SDF1. Ratios denote representative changes in nuclear (N) vs cytoplasmic (C) HuR. U1snRNP marks nuclear extracts and Actin is the loading control.

in chimeric thymi and diminished in the periphery of reconstituted mice (Fig. 3, *A* and *B*), suggesting defects in the generation of mature SP cells via positive selection. Cells undergoing selection are marked by an increase in surface TCR and CD5 levels and the transient expression of the early activation marker, CD69. *LckCre$^+$ Elavl1$^{fl/fl}$* DP cells contained a lesser number of HuR$^-$ cells initiating positive selection (TCRβ^{int}CD69^{high} or CD5^{high}) and, particularly, of cells undergoing positive selection (TCRβ^{high} CD69^{high} or CD5^{high}) (Fig. 3, *C* and *D*). Furthermore, the proliferative response of *LckCre$^+$ Elavl1$^{fl/fl}$* thymocytes to TCR agonists, but not mitogens, was reduced (Fig. 3*E*), suggesting defects in TCR signaling. This was exemplified further by the impaired activation of intracellular signals in HuR$^-$ thymocytes pulsed with TCR agonists. Although the protein levels of TCR adaptor and distal kinases like p56^{lck}, ZAP-70, and PKCθ remained unaltered in the absence of HuR, their phosphorylation was compromised in stimulated *Elavl1$^{Cre/-}$* thymocytes (Fig. 3*F*). Thus, HuR modulates TCR signals driving thymocyte positive selection.

HuR regulates chemokine signals driving thymocyte egress

A defect in positive selection could account for the loss of peripheral HuR$^-$ T cells but not for their presence as SP thymocytes. This paradox was also apparent in mice with TCR-transgenic thymocytes that recognize alloreactive MHC class I-restricted Ags like the F5-TCR that recognizes a viral Ag, or the HY-TCR recognizing the male autoantigen in female mice (supplemental Fig. 3). We note that HuR's loss was partial in *tgHY$^+$ LckCre$^+$ Elavl1$^{fl/fl}$* T cells, probably due to the surface expression of the HY-TCR in DN cells enforcing selection at the time of recombination of the *Elavl1* locus. Still, both systems suggested that HuR$^-$ SP cells accumulate in the thymus due to their defective egress. To test this, we labeled thymocytes via the intrathymic injection of FITC and analyzed peripheral naive (CD44^{low}) T cells for FITC$^+$ recent thymic emigrants (RTEs). In contrast to control groups, RTE counts were reduced in the periphery of *LckCre$^+$ Elavl1$^{fl/fl}$* mice (Fig. 4, *A* and *B*). In compliance with an impairment in egress, HuR$^-$ SP thymocytes were enriched in postselection TCRβ^+CD69^{low}CD62L^{high} cells (Fig. 4*C*) that respond to chemotactic signals for their intrathymic movements and accumulate in the presence of drugs inhibiting these processes (34). Such signals include those transduced by the shingosine-1-phosphate receptor 1 (S1P$_1$/EDG-1) acting through the Kruppel-like transcription factor 2, as well as the chemokine receptors CXCR4 and CCR7 (3, 4). The expression of these molecules was not altered in HuR$^-$ cells

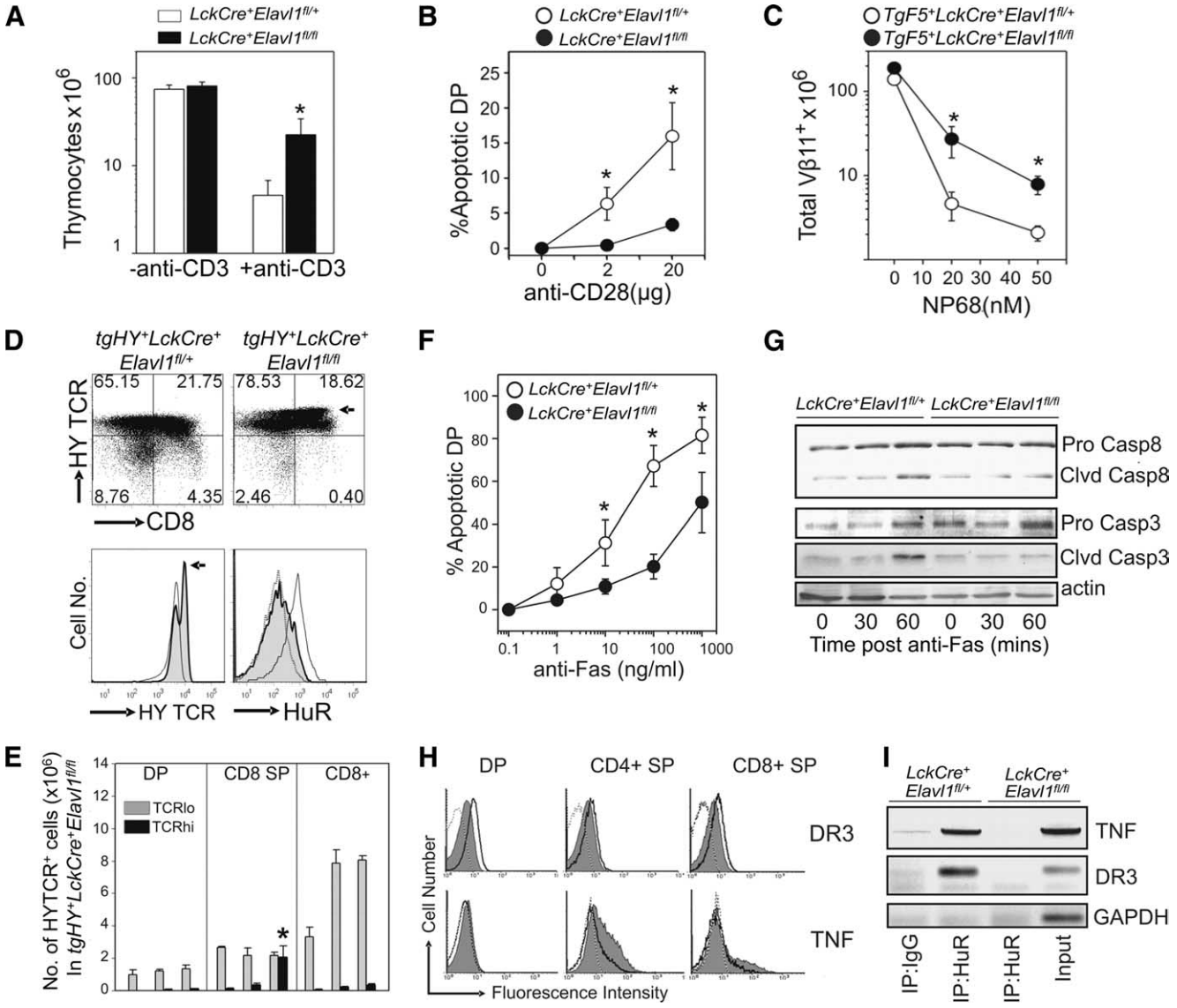

FIGURE 5. HuR$^-$ thymocytes show defects in Ag- and death receptor-induced deletion. *A*, Thymocyte counts (±SD) in control and *LckCre*$^+$ *Elavl1*$^{fl/fl}$ mice (n = 5–7) injected with anti-CD3. *B*, Ex vivo apoptotic response of control and *LckCre*$^+$ *Elavl1*$^{fl/fl}$ DP thymocytes to anti-CD3 and anti-CD28. Data (Annexin V$^+$ cells ± SD) from three independent experiments. ∗, $p < 0{,}01$. *C*, Counts of transgenic F5$^+$ thymocytes in 6-wk-old *F5*$^+$ *LckCre*$^+$ *Elavl1*$^{fl/fl}$ and control mice treated with increasing doses of their cognitive peptide. Data derived for n = 5 mice/group/dose. *D*, Detection of transgenic HY-TCR$^+$ in CD8$^+$SP from male *tgHY*$^+$ *LckCre*$^+$ *Elavl1*$^{fl/fl}$ and control thymi. Arrow indicates the presence of the HY-TCR^{high} subset. The histograms depict the levels of HY-TCR and HuR in thymocytes from control (*open histogram*) or test mice (*shaded histogram*) at the age of 15 wk. The arrow indicates the TCR^{high} signal. *Dotted line*, HuR's isotype staining. *E*, Counts of T cell subsets expressing low or high levels of the HY-TCR in male control or *TgHY*$^+$ *LckCre*$^+$ *Elavl1*$^{fl/fl}$ thymi and spleens (n = 7–10; ∗, $p < 0.01$). *F*, Apoptotic response of control and *Elavl1*$^{Cre/-}$ DP thymocytes to anti-Fas ligation. Data (±SD) are Annexin V$^+$ cells from four independent experiments. ∗, $p \leq 0.01$. *G*, Detection of pro- and cleaved caspase-8 and -3 in extracts from Fas-stimulated thymocytes. A representative of three experiments with actin as a loading control is shown. *H*, Intracellular detection of DR3 and TNF proteins in control (*open histogram*) and *LckCre*$^+$ *Elavl1*$^{fl/fl}$ (*filled histogram*) thymocytes relative to isotype background stains (*dotted line*). *I*, RT-PCR detection of TNF and DR3 mRNAs from HuR:R-IP assays using HuR$^+$ and HuR$^-$ thymocyte extracts; R-IP assays with IgG and inputs from HuR$^-$ extracts are also shown.

(supplemental Fig. 4) and the migration of HuR$^-$ and HuR$^+$ SP thymocytes to S1P was comparable (not shown). In contrast, HuR$^-$ SP thymocytes migrated poorly toward the CXCR4 ligand, CXCL12/SDF1, or the CCR7 ligand, CCL21 (Fig. 4*D*). Furthermore, these chemokines changed the subcellular distribution, but not the abundance of HuR in proficient thymocytes (supplemental Fig. 4). A prevalence of nuclear HuR was observed in CCL21-treated thymocytes, whereas the exact opposite was observed after SDF-1 treatment (Fig. 4*E*), suggesting that chemokines control HuR's functions differentially, for the optimal migration and egress of postselection SP thymocytes.

HuR regulates antigenic and death signals driving thymocyte deletion

The defective egress of HuR$^-$ SP thymocytes could also mask defects in thymocyte deletion, which is the basis of negative selection. This was suggested by the refractory response of HuR$^-$ DP thymocytes to anti-CD3-induced deletion in vivo and their defective ex vivo apoptotic response to anti-CD3 in the presence of anti-CD28 but not corticosteroids (Fig. 5, *A* and *B* and supplemental Fig. 5). Similarly, HuR's loss hindered Ag-induced deletion, as demonstrated by the poor elimination of F5-TCR$^+$HuR$^-$

Table I. *Priority list of differentially expressed genes in HuR-deficient thymocytes*

Rank[a]	Name	Gene ID[b]	Description	*p* Value[a]	Time[c]
Genes with reduced expression					
1	*Tnfrsf25*	85030	TNFR superfamily, member 25	0.002678	0
2	*Ssrp1*	20833	Structure-specific recognition protein 1	0.006325	0
3	*Lta*	16992	Lymphotoxin-α precursor	0.017035	0
4	*Rbm5*	83486	RNA binding motif protein 5	0.023424	4
5	*Sorbs1*	20411	Sorbin and Sh3 domain containing 1	0.034589	4
6	*Flt4*	14257	VEGF receptor 3 precursor	0.034667	0
7	*Toe1*	68276	Target of Egr1, member 1	0.048476	4
Genes with increased expression					
1	*Runx1*	12394	Runt-related transcription factor 1	4.9 E-04	12
2	*Stat3*	20848	Signal transducer and activator of transcription 3	0.001066	12
3	*Vav1*	22324	Vav proto-oncogene	0.001552	4
4	*Tnf*	21926	Tumor necrosis factor precursor (TNF-α)	0.007034	12
5	*Sfrs2*	20382	Splicing factor, arginine/serine-rich 2	0.011264	12
6	*Nfkbie*	18037	NF-κB inhibitor ϵ (Iκ-Bϵ)	0.01673	12
7	*Dnmt1*	13433	DNA methyltransferase (cytosine-5) 1	0.017911	12
8	*Sla*	20491	Src-like adaptor protein	0.01804	12
9	*Cd2*	12481	T cell surface antigen Cd2 precursor (Lfa-2)	0.01876	12
10	*Cd3e*	12501	T cell surface glycoprotein Cd3 ϵ-chain precursor	0.030197	4
11	*Ppp4c*	56420	Protein phosphatase 4, catalytic subunit	0.0318	4
12	*Akt3*	23797	Protein kinase Akt-3; (Protein kinase B, γ)	0.035526	4
13	*Cdc25a*	12530	M-phase inducer phosphatase 1	0.03866	4
14	*Jarid2*	16468	Jumonji, at rich interactive domain 2	0.040707	12
15	*Cdc25b*	12531	M-phase inducer phosphatase 2	0.043261	12

[a] Ranking and corresponding *p* values based on Endeavour prioritization for down-regulated or up-regulated genes relating to enlarged thymus.
[b] Entrez Gene IDs.
[c] Time when differential expression was detected (prior/after stimulation).

thymocytes exposed to a chronic 4-day administration regime of their cognitive NP68 peptide (Fig. 5*C* and supplemental Fig. 5). To extend our observations to autoantigen-induced deletion, we analyzed the elimination of autoreactive HY-TCR$^+$ transgenic thymocytes, which occurs in male mice. We hypothesized that because HuR$^-$ HY-TCR$^+$ thymocytes were partially present in *tgHY*$^+$ *LckCre*$^+$ *Elavl1*$^{fl/fl}$ female mice, presumptive defects in their deletion and egress should enforce their presence in the autoreactive male environment. In control males, HY-TCR$^+$ DP thymocytes were consistently deleted, whereas remnant CD8$^+$ SPs possessed an anergic HY-TCR^{low} phenotype. Contrastingly, and despite the early loss of DP thymocytes in *tgHY*$^+$ *LckCre*$^+$ *Elavl1*$^{fl/fl}$ thymi, a HuR$^-$HY-TCR^{high} CD8$^+$ SP subset emerged at 5 wk of age and accounted for a 50% increase in total CD8$^+$ SP thymocytes by 15 wk of age (Fig. 5, *D* and *E* and supplemental Fig. 5). Strikingly, peripheral CD8$^+$ HuR$^-$ HY-TCR^{high} subsets could not be detected in *tgHY*$^+$ *LckCre*$^+$ *Elavl1*$^{fl/fl}$ mice (Fig. 5*E*), demonstrating that the loss of HuR hinders the deletion of autoreactive thymocytes but does not allow their exiting from the thymus.

Thymocyte deletion is influenced by proapoptotic signals emanating from death receptors like Fas (CD95/Apo-1), which supports clonal deletion at high-Ag concentrations (35). The expression of Fas was not altered in *LckCre*$^+$ *Elavl1*$^{fl/fl}$ thymocytes (supplemental Fig. 5), but these cells showed a minimal apoptotic response to anti-Fas ligation and a consistent lack of cleaved caspases-8 and -3 (Fig. 5, *F* and *G*). Collectively, HuR is required for Ag and death-receptor induced thymocyte deletion.

HuR controls gene networks supporting thymocyte maturation

To identify gene networks affected by HuR's dysfunction, we performed microarray hybridizations using RNA from control and HuR$^-$ thymocytes stimulated for 0, 4, and 12 h by mitogens. Two hundred forty one unique RNAs were identified as differentially up (140) or down (101) in HuR$^-$ thymocytes (Supplemental Table I, a and b). Some of the previously reported HuR-target mRNAs (e.g., cyclins, cytokines, and transcription factors) were expressed in thymocytes, but appeared unaffected by HuR's loss (Supplemental Fig. 6). To relate the expression data to the phenotypes of HuR$^-$ thymocytes, we used the Endeavour relational software to perform a computational prioritization of differentially expressed genes (Table I) based on a training set of 177 genes (supplemental Tables) controlling thymic cellularity. The hyperproliferation of HuR$^-$ DN thymocytes, related to the increased expression of Cdc25A/B phosphatases which promote cell cycle progression. Defects in antigenic signaling related to increases in mRNAs encoding the TCR constituents and downstream signalers (*CD2, CD3*ε*, Vav1, Act3, Runx1*) but also to decreases in the mRNA of the Src-like adaptor protein Sla, which inhibits CD3ζ-signaling in DP cells and the *Toe-1* mRNA, which is a target of the Egr-1 transcription factor required for positive selection. Most strikingly, the defective deletion of HuR$^-$ thymocytes related to changes in members of the TNF/TNFR family. Subsequent analyses validated the direct involvement of HuR in the modulation of such molecules. The biosynthesis of TNF-α was augmented in activated HuR$^-$ thymocytes, whereas its mRNA was associated with thymocyte HuR in R-IP assays (Fig. 5, *H* and *I* and supplemental Fig. 5), confirming previous observations on HuR's negative control over TNF biosynthesis (10). In light of TNF's positive role in thymocyte deletion (36), and the invariable expression of its receptors in HuR$^-$ thymocytes (supplemental Fig. 5 and not shown), we postulate that HuR affects downstream TNFR signaling as in the case of Fas. In contrast, however, to TNFRs and Fas, the expression of *TNFRSF25/DR3*, which promotes negative selection (37), was reduced in HuR$^-$ thymocytes and particularly in DP cells. Most importantly, the *DR3* mRNA precipitated with thymocyte HuR in HuR-R-IP assays (Fig. 5, *H* and *I* and supplemental Fig. 5), suggesting that HuR can control both proximal and distal proapoptotic signals. Collectively, our profiling data connect HuR's control over thymocyte

maturation to gene expression programs controlling cell cycle, TCR, and TNFR/death receptor signaling.

Discussion

In this report, we revealed HuR's pleiotropic control over TCR$\alpha\beta^+$ T cell development via its genetic ablation in thymocyte precursors. On the one end, HuR's loss caused an increase in thymic cellularity due to hyperproliferating DN cells, nondeleted thymocytes, and the nonmigrating mature T cells. On the other end, the loss of peripheral HuR$^-$ T cells was attributed to their defective positive selection and the defective egress of remnant cells. These aberrations reflected HuR's involvement in thymocyte intrinsic/extrinsic signals that could only be revealed in an in vivo multiparametric context.

The hyperproliferation of HuR$^-$ DN thymocytes highlighted HuR's role as a cell cycle suppressor of pre-T cells undergoing β-selection. HuR's involvement in cell-cycle control has been inferred previously via its affinity for mRNAs encoding cyclins, tumor suppressors, proto-oncogenes, Cdk inhibitors, and enzymes promoting DNA repair, as well as apoptotic modulators (15, 38). In our study, the increased proliferation of HuR$^-$ DN cells related to their reduced content in one of HuR's known targets, p53, which plays a dominant role toward the growth arrest of pre-T cells undergoing β-selection. In the absence of a functional pre-TCR, p53 accumulates to aid cell clearance by apoptosis, whereas productive TCRβ rearrangements inactivate p53, resulting in cell cycle entry. *p53*^{null} DN thymocytes escape this checkpoint and become DP even in the absence of a functional pre-TCR (39). This role for p53 may also apply for HuR$^-$ thymocytes, as suggested by the increased expression of Cdc25A and B phosphatases, which promote G1/S-phase transition and activation of the mitotic Cdk1/cyclin B complex. Similar changes in Cdc25 expression have been reported in *p53*^{null} cells (40) and p53 is known to repress the transcription of Cdc25 genes (41, 42). Consistent with HuR's role in promoting *p53* mRNA translation (12), we propose that HuR may enhance the expression of p53 to promote cell cycle arrest in DN thymocytes. However, the reduction of p53 protein in HuR$^-$ DN thymocytes may also result from alterations in its posttranslational modifications controlling its stability (43); this points toward HuR's alternative involvement in signals guiding p53's modification and cell cycle control. Consistent with this suggestion, prior data demonstrated that HuR can be phosphorylated by the checkpoint kinase Chk2 to bind to its targets during oxidative stress (15) and that Chk2 contributes to the stabilization of p53 (44). Conversely, HuR functions can be blocked by its nuclear retention following phosphorylation by Cdk1 (16), whereas Cdk1 is inhibited by p53 and p21 (45).

The prevalence of HuR$^-$ DN cells was counteracted by the lack of TCR signals needed for positive selection. Because antigenic/TCR signals alter the abundance and localization of HuR in T cells, we postulate that they converge to HuR to control its functions for the prudent execution of gene expression programs driving thymocyte activation during positive selection. This supposition is supported further by the efficacy of a small molecule inhibitor of HuR's shuttling that blocks T cell activation in vitro (46).

Alternatively, HuR may also affect the expression of TCR signalers, as suggested by the loss of proximal TCR signaling in HuR$^-$ cells. Our profiling data provided important clues for HuR's interference to TCR signaling by the altered expression of TCR constituents or their regulators, like the CD3ε-associated molecule Sla in HuR$^-$ cells, which is known to block the signaling functions of CD3ζ (47). Supporting our hypothesis is a parallel study identifying mRNA targets of HuR that change during T cell activation in Jurkat cells, and encode proteins imminent to TCR signaling (N. Mukherjee and J. D. Keene, submitted for publication).

HuR's requirement in TCR signaling was substantiated further by the defective deletion of HuR$^-$ thymocytes, because a reduction in the thresholds of (auto)antigenic signaling could account for this effect. However, HuR is also involved in extrinsic, proapoptotic, cytokine signals such as those induced by Fas or other TNFR family members like TNFRI or DR3. Thus, HuR can modulate proapoptotic cytokine signaling in two ways. It can bind and affect the expression of apoptotic ligands (e.g., TNF) or death receptors (e.g., DR3). Adding to our data, a recent biochemical report showed that HuR can promote the alternative splicing of *Fas* pre-RNA to encode for its transmembrane rather than its soluble isoform (21). Although HuR$^-$ thymocytes expressed normal levels of intracellular and transmembrane Fas protein, we cannot exclude the possible overproduction of soluble Fas as an additional mechanism affecting in vivo thymocyte deletion. On top of its biosynthetic effect on ligands/receptors, HuR's involvement in proapoptotic signals can be inferred by the sharing of signal transducers from DR3, Fas, and TNFRI (48, 49). How can HuR interfere with these signals? A recent report (18) demonstrated that, during lethal challenge, HuR is cleaved at an aspartate residue by a mechanism requiring caspase-7 and -3. Cleavage releases HuR from its translocation partner pp32/PHAP-I, which then acts as a proapoptotic factor by stimulating the activity of the apoptosome complex. In our study, cleaved HuR was detected in TCR- or Fas-stimulated thymocytes, suggesting that its absence may block the activation of the apoptosome during thymocyte deletion. However, HuR's cleavage was also induced during corticosteroid-induced thymocyte deletion, which was not affected by HuR's loss. Furthermore, the refractory response of HuR$^-$ thymocytes to Fas related to the defective activation of upstream caspase-8. Thus, it seems that HuR controls both upstream proapoptotic signals as well as the activation of the apoptosome.

The loss of HuR's control over thymocyte egress caused the accumulation of postselection HuR$^-$ SP thymocytes and the reduction in peripheral HuR$^-$ RTEs. Two chemokine-dependant processes have been linked to egress of mature thymocytes: 1) their CCR7- or CXCR4-dependent retention/repulsion toward the medullary endothelial cells, and 2) their S1PR-dependent attraction toward the peripheral blood. HuR$^-$ SP thymocytes showed a compromised response only to CXCR4 and CCR7 ligands, suggesting that HuR controls medullary movements and not thymocyte attraction to the peripheral blood. This could also provide an explanation as to why egress is not fully blocked as in cases of S1PR blockade (50). Similarly, the differential cytoplasmic response of HuR to CXCR4 and CCR7 ligands may reflect its differential involvement in cellular retention vs repulsion.

At the molecular level, we postulate that HuR acts both as a regulator of gene expression and as a modulator of signal transduction. Given the diversity of T cell phenotypes and responses, a subset/signal restricted analysis on proteomic/ribonomic interactions needs to be performed to reveal the complete HuR "interact-ome" in T cells. Clearly however, our data are against the simplistic dogma where HuR acts to control the use of mRNAs in a common manner because the limited number of HuR-interacting mRNAs examined herein show variable responses to HuR's absence. We note however the observed changes in these mRNAs may either reflect differences in mRNA stability/translation relating to direct HuR functions or extent to other direct/indirect transcriptional/posttranscriptional processes including the functions of other RBPs.

Finally, and in the context of adaptive immunity, many of the thymocytic signals affected by HuR's dysfunction are also implicated in peripheral T cell responses under physiological or inflammatory settings. In that context, the peripheral T cell loss observed in mutant mice could also results from defects in peripheral subset

composition, activation, proliferation, and survival. Similarly, and based on our findings on the control of thymocyte deletion of autoreactive thymocytes, HuR could affect negative selection as well as peripheral tolerance to auto- or innocuous Ags and autoimmunity. These important immunological processes will be examined in the future, along with the combined effects of HuR, other RBPs, and noncoding regulatory RNAs on adaptive immunity.

Acknowledgments

Thanks to V. Katsanou for her contributions at the early stages of this project; P. J. Lager for his support in the microarray experiments; A. Potocnik for training on intrathymic FITC injections, CD45.1 congenic strains, and comments; D. Kioussis, B. Malissen, and G. Kollias for mice; and G. Kassiotis, C. Mamalaki, M. Apostolaki, and D. Graf for critical discussions and comments.

Disclosures

The authors have no financial conflict of interest.

References

1. Bassing, C. H., W. Swat, and F. W. Alt. 2002. The mechanism and regulation of chromosomal V(D)J recombination. *Cell* 109: S45–S55.
2. Starr, T. K., S. C. Jameson, and K. A. Hogquist. 2003. Positive and negative selection of T cells. *Annu. Rev. Immunol.* 21: 139–176.
3. Jin, R., J. Zhang, and W. Chen. 2006. Thymic output: influence factors and molecular mechanism. *Cell. Mol. Immunol.* 3: 341–350.
4. Takahama, Y. 2006. Journey through the thymus: stromal guides for T-cell development and selection. *Nat. Rev. Immunol.* 6: 127–135.
5. Cheadle, C., J. Fan, Y. S. Cho-Chung, T. Werner, J. Ray, L. Do, M. Gorospe, and K. G. Becker. 2005. Control of gene expression during T cell activation: alternate regulation of mRNA transcription and mRNA stability. *BMC. Genomics.* 6: 75–80.
6. Keene, J. D. 2007. RNA regulons: coordination of post-transcriptional events. *Nat. Rev. Genet.* 8: 533–543.
7. Khabar, K. S. 2005. The AU-rich transcriptome: more than interferons and cytokines, and its role in disease. *J. Interferon Cytokine Res.* 25: 1–10.
8. Keene, J. D. 1999. Why is Hu where? Shuttling of early-response-gene messenger RNA subsets. *Proc. Natl. Acad. Sci. USA* 96: 5–7.
9. Gallouzi, I. E., and J. A. Steitz. 2001. Delineation of mRNA export pathways by the use of cell-permeable peptides. *Science* 294: 1895–1901.
10. Katsanou, V., O. Papadaki, S. Milatos, P. J. Blackshear, P. Anderson, G. Kollias, and D. L. Kontoyiannis. 2005. HuR as a negative posttranscriptional modulator in inflammation. *Mol. Cell.* 19: 777–789.
11. Kullmann, M., U. Gopfert, B. Siewe, and L. Hengst. 2002. ELAV/Hu proteins inhibit p27 translation via an IRES element in the p27 5′UTR. *Genes Dev.* 16: 3087–3099.
12. Mazan-Mamczarz, K., S. Galban, I. Lopez de Silanes, J. L. Martindale, U. Atasoy, J. D. Keene, and M. Gorospe. 2003. RNA-binding protein HuR enhances p53 translation in response to ultraviolet light irradiation. *Proc. Natl. Acad. Sci. USA* 100: 8354–8359.
13. Bhattacharyya, S. N., and W. Filipowicz. 2007. Argonautes and company: sailing against the wind. *Cell* 128: 1027–1028.
14. Keene, J. D., and S. A. Tenenbaum. 2002. Eukaryotic mRNPs may represent posttranscriptional operons. *Mol. Cell.* 9: 1161–1167.
15. Gorospe, M., and R. de Cabo. 2008. AsSIRTing the DNA damage response. *Trends Cell Biol.* 18: 77–83.
16. Kim, H. H., K. Abdelmohsen, A. Lal, R. Pullmann, Jr., X. Yang, S. Galban, S. Srikantan, J. L. Martindale, J. Blethrow, K. M. Shokat, and M. Gorospe. 2008. Nuclear HuR accumulation through phosphorylation by Cdk1. *Genes Dev.* 22: 1804–1815.
17. Li, H., S. Park, B. Kilburn, M. A. Jelinek, A. Henschen-Edman, D. W. Aswad, M. R. Stallcup, and I. A. Laird-Offringa. 2002. Lipopolysaccharide-induced methylation of HuR, an mRNA-stabilizing protein, by CARM1: coactivator-associated arginine methyltransferase. *J. Biol. Chem.* 277: 44623–44630.
18. Mazroui, R., S. Di Marco, E. Clair, C. von Roretz, S. A. Tenenbaum, J. D. Keene, M. Saleh, and I. E. Gallouzi. 2008. Caspase-mediated cleavage of HuR in the cytoplasm contributes to pp32/PHAP-I regulation of apoptosis. *J. Cell Biol.* 180: 113–127.
19. Atasoy, U., J. Watson, D. Patel, and J. D. Keene. 1998. ELAV protein HuA (HuR) can redistribute between nucleus and cytoplasm and is upregulated during serum stimulation and T cell activation. *J. Cell Sci.* 111: 3145–3156.
20. Casolaro, V., X. Fang, B. Tancowny, J. Fan, F. Wu, S. Srikantan, S. Y. Asaki, U. De Fanis, S. K. Huang, M. Gorospe, U. X. Atasoy, and C. Stellato. 2008. Posttranscriptional regulation of IL-13 in T cells: role of the RNA-binding protein HuR. *J. Allergy Clin. Immunol.* 121: 853–859.
21. Izquierdo, J. M. 2008. Hu antigen R (HuR) functions as an alternative pre-mRNA splicing regulator of Fas apoptosis-promoting receptor on exon definition. *J. Biol. Chem.* 283: 19077–19084.
22. Moulton, V. R., V. C. Kyttaris, Y. T. Juang, B. Chowdhury, and G. C. Tsokos. 2008. The RNA-stabilizing protein HuR regulates the expression of zeta chain of the human T cell receptor-associated CD3 complex. *J. Biol. Chem.* 283: 20037–20044.
23. Sakai, K., Y. Kitagawa, M. Saiki, S. Saiki, and G. Hirose. 2003. Binding of the ELAV-like protein in murine autoimmune T-cells to the nonameric AU-rich element in the 3′ untranslated region of CD154 mRNA. *Mol. Immunol.* 39: 879–883.
24. Wang, J. G., M. Collinge, V. Ramgolam, O. Ayalon, X. C. Fan, R. Pardi, and J. R. Bender. 2006. LFA-1-dependent HuR nuclear export and cytokine mRNA stabilization in T cell activation. *J. Immunol.* 176: 2105–2113.
25. Yarovinsky, T. O., N. S. Butler, M. M. Monick, and G. W. Hunninghake. 2006. Early exposure to IL-4 stabilizes IL-4 mRNA in CD4+ T cells via RNA-binding protein HuR. *J. Immunol.* 177: 4426–4435.
26. Katsanou, V., S. Milatos, A. Yakouvaki, N. Sgantzis, A. Kotsoni, M. Alexiou, V. Harokopos, V. Aidinis, M. Hemberger, and D. Kontoyiannis. 2009. The RNA-binding protein Elavl1/HuR is essential for placental branching morphogenesis and embryonic development. *Mol. Cell Biol.* March 23. E-pub ahead of print.
27. Orban, P. C., D. Chui, and J. D. Marth. 1992. Tissue- and site-specific DNA recombination in transgenic mice. *Proc. Natl. Acad. Sci. USA* 89: 6861–6865.
28. Mamalaki, C., J. Elliott, T. Norton, N. Yannoutsos, A. R. Townsend, P. Chandler, E. Simpson, and D. Kioussis. 1993. Positive and negative selection in transgenic mice expressing a T-cell receptor specific for influenza nucleoprotein and endogenous superantigen. *Dev. Immunol.* 3: 159–174.
29. Tarazona, R., O. Williams, D. Moskophidis, L. A. Smyth, Y. Tanaka, M. Murdjeva, A. Wack, C. Mamalaki, and D. Kioussis. 1998. Susceptibility and resistance to antigen-induced apoptosis in the thymus of transgenic mice. *J. Immunol.* 160: 5397–5403.
30. Kisielow, P., H. Bluthmann, U. D. Staerz, M. Steinmetz, and H. von Boehmer. 1988. Tolerance in T-cell-receptor transgenic mice involves deletion of nonmature CD4+8+ thymocytes. *Nature* 333: 742–746.
31. Staton, T. L., B. Johnston, B. Butcher, and D. J. Campbell. 2004. Murine CD8+ Recent Thymic emigrants are αE and integrin-positive and CC chemokine Ligand 25 Responsive. *J. Immunol.* 172: 7282–7288.
32. Campbell, J. J., S. Qin, K. B. Bacon, C. R. Mackay, and E. C. Butcher. 1996. Biology of chemokine and classical chemoattractant receptors: differential requirements for adhesion-triggering versus chemotactic responses in lymphoid cells. *J. Cell Biol.* 134: 255–266.
33. Wang, W., H. Furneaux, H. Cheng, M. C. Caldwell, D. Hutter, Y. Liu, N. Holbrook, and M. Gorospe. 2000. HuR regulates p21 mRNA stabilization by UV light. *Mol. Cell. Biol.* 20: 760–769.
34. Kurobe, H., C. Liu, T. Ueno, F. Saito, I. Ohigashi, N. Seach, R. Arakaki, Y. Hayashi, T. Kitagawa, M. Lipp, R. L. Boyd, and Y. Takahama. 2006. CCR7-dependent cortex-to-medulla migration of positively selected thymocytes is essential for establishing central tolerance. *Immunity* 24: 165–177.
35. Kishimoto, H., C. D. Surh, and J. Sprent. 1998. A role for Fas in negative selection of thymocytes in vivo. *J. Exp. Med.* 187: 1427–1438.
36. Page, D. M., E. M. Roberts, J. J. Peschon, and S. M. Hedrick. 1998. TNF receptor-deficient mice reveal striking differences between several models of thymocyte negative selection. *J. Immunol.* 160: 120–133.
37. Wang, E. C., A. Thern, A. Denzel, J. Kitson, S. N. Farrow, and M. J. Owen. 2001. DR3 regulates negative selection during thymocyte development. *Mol. Cell. Biol.* 21: 3451–3461.
38. Brennan, C. M., and J. A. Steitz. 2001. HuR and mRNA stability. *Cell. Mol. Life Sci.* 58: 266–277.
39. Haks, M. C., P. Krimpenfort, J. H. van den Brakel, and A. M. Kruisbeek. 1999. Pre-TCR signaling and inactivation of p53 induces crucial cell survival pathways in pre-T cells. *Immunity* 11: 91–101.
40. Aressy, B., B. Bugler, A. Valette, D. Biard, and B. Ducommun. 2008. Moderate variations in CDC25B protein levels modulate the response to DNA damaging agents. *Cell Cycle* 7: 2234–2240.
41. Rother, K., R. Kirschner, K. Sanger, L. Bohlig, J. Mossner, and K. Engeland. 2007. p53 downregulates expression of the G1/S cell cycle phosphatase Cdc25A. *Oncogene* 26: 1949–1953.
42. St Clair, S., and J. J. Manfredi. 2006. The dual specificity phosphatase Cdc25C is a direct target for transcriptional repression by the tumor suppressor p53. *Cell Cycle* 5: 709–713.
43. Murray-Zmijewski, F., E. A. Slee, and X. Lu. 2008. A complex barcode underlies the heterogeneous response of p53 to stress. *Nat. Rev. Mol. Cell Biol.* 9: 702–712.
44. Hirao, A., Y. Y. Kong, S. Matsuoka, A. Wakeham, J. Ruland, H. Yoshida, D. Liu, S. J. Elledge, and T. W. Mak. 2000. DNA damage-induced activation of p53 by the checkpoint kinase Chk2. *Science* 287: 1824–1827.
45. Satyanarayana, A., M. B. Hilton, and P. Kaldis. 2008. p21 inhibits Cdk1 in the absence of Cdk2 to maintain the G1/S phase DNA damage checkpoint. *Mol. Biol. Cell* 19: 65–77.
46. Meisner, N. C., M. Hintersteiner, K. Mueller, R. Bauer, J. M. Seifert, H. U. Naegeli, J. Ottl, L. Oberer, C. Guenat, S. Moss, et al. 2007. Identification and mechanistic characterization of low-molecular-weight inhibitors for HuR. *Nat. Chem. Biol.* 3: 508–515.
47. Myers, M. D., T. Sosinowski, L. L. Dragone, C. White, H. Band, H. Gu, and A. Weiss. 2006. Src-like adaptor protein regulates TCR expression on thymocytes by linking the ubiquitin ligase c-Cbl to the TCR complex. *Nat. Immunol.* 7: 57.
48. Chinnaiyan, A. M., K. O'Rourke, G. L. Yu, R. H. Lyons, M. Garg, D. R. Duan, L. Xing, R. Gentz, J. Ni, and V. M. Dixit. 1996. Signal transduction by DR3, a death domain-containing receptor related to TNFR-1 and CD95. *Science* 274: 990–992.
49. Wen, L., L. Zhuang, X. Luo, and P. Wei. 2003. TL1A-induced NF-κB activation and c-IAP2 production prevent DR3-mediated apoptosis in TF-1 cells. *J. Biol. Chem.* 278: 39251–39258.
50. Matloubian, M., C. G. Lo, G. Cinamon, M. J. Lesneski, Y. Xu, V. Brinkmann, M. L. Allende, R. L. Proia, and J. G. Cyster. 2004. Lymphocyte egress from thymus and peripheral lymphoid organs is dependent on S1P receptor 1. *Nature* 427: 355–360.